ELSEVIER

Surface Science 388 (1997) L1121–L1125

surface science

Surface Science Letters

Sputter deposition of atomically flat Au(111) and Ag(111) films

Mitsuo Kawasaki *, Hideki Uchiki

Department of Molecular Engineering, Graduate School of Engineering, Kyoto University, Yoshida, Kyoto 606-01, Japan

Received 24 March 1997; accepted for publication 24 June 1997

Abstract

A simple Ar-ion sputter deposition has allowed preparation of atomically flat Au(111) and Ag(111) films in conditions of much lower substrate temperature and/or deposition rate compared with vacuum deposition. At a deposition rate less than 1 Å s^{-1}, Au(111) films with extended terrace structures could be grown on a freshly cleaved and heated mica (~300°C) without extensive substrate prebaking. Sputtered Ag(111) films could also be grown atomically flat at a similar deposition rate, preferably on Au(111) predeposited on mica. Particularly smooth Ag(111) films often accompanied by hexagonal faceting grew at substrate temperatures, 150–200°C, near the point at which serious clouding of the film surface set in. © 1997 Elsevier Science B.V.

Keywords: Epitaxy; Gold; Scanning tunneling microscopy; Silver; Sputter deposition; Surface morphology

The fascinating capability of scanning tunneling microscopy (STM) and/or atomic force microscopy (AFM) to allow atomic-resolution imaging of a variety of organic and biological structures rests upon whether or not such structures can be firmly fixed on a suitable substrate [1,2], which must be electrically conducting (for STM) and should have sufficiently large, homogeneous, and atomically flat areas. As such a substrate, thin Au(111) films grown epitaxially on heated mica have gained much popularity, as they can be grown relatively easily by conventional vacuum evaporation and the Au surface exhibits strong affinity with, for example, organothiols and analogous sulfur compounds [3–7]. In this connection, a number of STM and AFM studies have been published on the optimum Au deposition conditions that promise an atomic-scale flatness extending over the required macroscopic area [8–13]. An extensive characterization of the epitaxial growth of Ag(111) on mica, closely related to that of Au(111), has also been reported by Baski and Fuchs [14]. However, all of these works primarily concern evaporated Au(111) or Ag(111) films, and the general deposition criteria deduced therein do not necessarily apply to other possible methods. Here we demonstrate this by introducing markedly smooth and well-oriented Au(111) films DC-sputtered onto mica and also atomically flat Ag(111) films sputtered onto the Au(111) film predeposited on mica. The method employed here is much simpler than vacuum evaporation in terms of both instrumentation and deposition procedure. Still, with the key deposition parameters properly chosen for the given system, the sputtered films exhibit superior surface planarity, even flatter than the smoothest evaporated films reported to date, particularly in the case of Ag(111) film. We have already used such Ag(111) films grown in a similar

* Corresponding author. Fax: (+81) 75 753.5526; e-mail: kawasaki@ap6.kuic.kyoto-u.ac.jp

0039-6028/97/$17.00 © 1997 Published by Elsevier Science B.V. All rights reserved.
PII S0039-6028(97)00516-5

SURFACE SCIENCE LETTERS

manner in some of our previous work to construct a model AgX surface for simulating of, for example, the formation of various dye aggregates on AgX as well as its surface atomic structure [15–17]. The films presently available and reported in this paper are a great improvement on those previous films and show the level of flatness that we hardly thought could be made by a simple sputtering technique.

All depositions were made in a relatively small-sized sputter-coating apparatus (Nippon Denshi, JFC-1100). The apparatus has been remodeled in this laboratory to allow DC discharge in a pure Ar atmosphere and heating of the sample with a tabular ($15 \times 55 \times 3$ mm^3) ~20 W ceramic heater (Kyocera Corporation, SP-20). A sheet of natural mica (as obtained from The Nilaco Corporation) cut to the size of typically 25×40 mm^2 was freshly cleaved to ~0.1 mm thick and clamped against an Al plate ($30 \times 45 \times 3$ mm^3). As illustrated in Fig. 1, this sample assembly was simply leaned against the ceramic heater on a thin metallic support, thereby the rear surface of the Al plate made direct contact with the ceramic heater in a slightly (by ~5°) tilted vertical configuration ~1 cm away from the edge of the target (99.99% gold or silver thin plate 45 mm in diameter) fixed horizontally at the bottom of the deposition chamber. Pumping of the deposition chamber (~3 dm^3 in inner volume) was done by using a standard rotary pump with which the highest vacuum attainable was ~10^{-3} Torr at best. It should be noted, however, that combined use of a turbo molecular pump in an attempt to ensure much higher vacuum, at least in the period of substrate preheating, did not produce any improvement in the flatness of the sputtered film. The cleanliness of the system and the substrate surface seemed to be ensured more effectively by continuously flowing the pure (99.999%) Ar gas throughout the whole process, including substrate preheating and postdeposition cooling back to the room temperature. It should also be noted that, in contrast to vacuum evaporation for which the importance of quite a lengthy (more than several hours) preheating of mica at temperatures as high as ~500°C has been addressed [11], the corresponding step in our experiment typically lasted for only ~30 min, which is just the time required to bring the substrate to the steady-state deposition temperature. During the DC discharge at the Ar gas pressure of 0.15–0.2 Torr, as measured by a Pirani gauge, the steady-state Ar-gas flow rate (equal to the pumping rate adjusted by the outlet valve control) was maintained as small as ~1.5 ml min^{-1}. The choice of this small Ar-gas flow rate seemed rather critical for producing highly planar sputtered films, while a little more flexible choice seemed to be allowed with respect to the discharge pressure. In these gas-phase conditions, the deposition rate was controlled by the cathode voltage (~0.9 kV negative at the standard condition), which in turn determined the total discharge current (~8 mA). It should also be noted that, in the aforementioned sample configuration relative to the target (see Fig. 1), the local deposition rate on the substrate was subject to a noticeable gradation from top to bottom. A typical average deposition rate, as estimated by weighing the total mass of the deposit, was ~40 Å min^{-1} (a little less than 1 Å s^{-1}). The substrate temperature was estimated in repeated parallel experiments with a chromel–alumel thermocouple contacted directly with the substrate surface in conditions otherwise identical to those used in actual sample preparations. We estimate the typical error here to be around ±10% on the celsius scale. The surface morphology and topo-

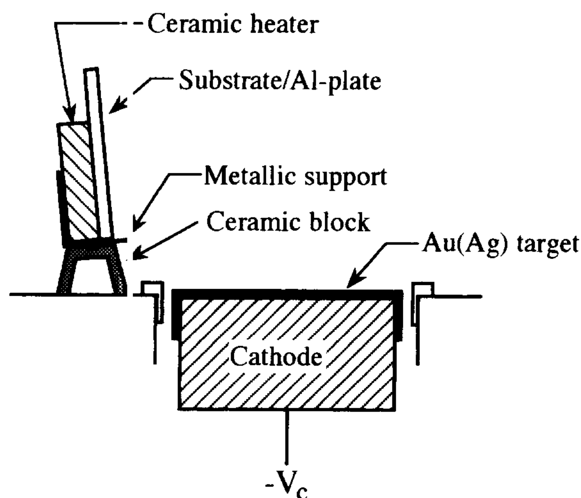

Fig. 1. Sample set-up and configuration inside the sputter-deposition chamber.

graphic feature of the sputtered films were examined by STM. The images were taken in air by using a Nanoscope-I microscope (Digital Instruments, Inc.) in the constant current mode with a Pt/Ir tip. All the images reported in this paper were obtained at negative sample bias of −100 mV and tunneling current of 0.5–0.8 nA.

The variable parameter space for the sputter deposition may be so large that we have not necessarily reached the real optimum deposition condition yet. Even so, in around our standard deposition conditions described above, atomically smooth Au(111) films typically 150–200 nm thick (exclusive (111) orientation of the sputtered films was confirmed by X-ray diffraction in previous work [15]) could be grown in a relatively wide temperature range above ~250°C up to the highest temperature (~350°C) examined; we did not go any higher than this for system protection from potential thermal damage. It should also be noted that a noticeable improvement in flatness was observed by allowing the main deposition step to be followed by a considerably slower secondary deposition at ~4 Å min^{-1} for approximately 20 min. Fig. 2 shows some typical examples of wide-scan (1500–2500 nm across) STM images taken for the resultant Au(111) films. All the images exhibit an extensively terraced structure, with either rounded step edges or hexagonal facet steps characteristic of (111) planes of fcc metals. The majority of the steps separating the individual terraces, some hundreds of nanometers in width, measured ~2.5 Å in height, as expected for monatomic steps (2.35 Å) on Au(111) planes. In addition, the large-scale hexagonal faceting visible in the widest 2500 nm image (Fig. 2a) suggests that the Au(111) film is also well oriented in the lateral direction over an area more than a few millimeters in width. Thus, in almost every aspect, our sputtered Au(111) films compare favorably with the smoothest evaporated films that have been reported to grow on an extensively prebaked mica and at notably higher deposition temperatures well exceeding 400°C [11]. It has also been suggested that higher deposition rates produce flatter films for evaporated Au growth on mica [10]. This criterion seems not to apply to the present case, because the deposition rate used here (less than 1 Å s^{-1}) is comparatively smaller than those (1–10 Å s^{-1}) typically used for vacuum deposition.

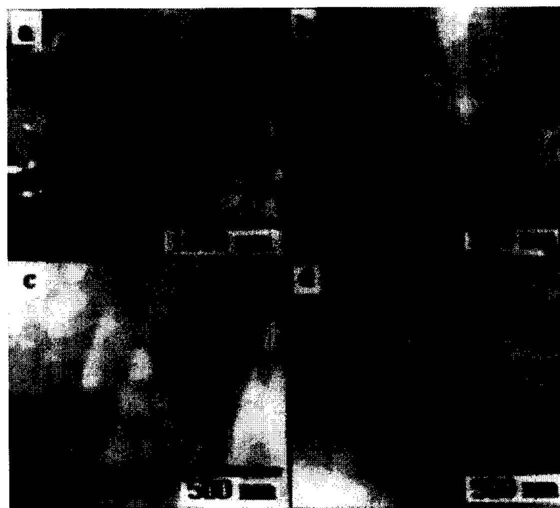

Fig. 2. A variety of wide-scan STM images taken for ~200 nm thick Au(111) films sputter grown on mica at a substrate temperature of ~300°C in the otherwise standard deposition conditions described in the text. Image (b) is a 1500 nm zoom in the same region as imaged in (a), whereas images (c) and (d) were taken in different regions of the sample. The apparent maximum height differences between the brightest and darkest parts of each image are: (a) 5.7 nm, (b) 2.8 nm, (c) 3.0 nm, (d) 2.5 nm.

The Ag(111) films were overgrown epitaxially for a thickness of 50–100 nm on the already atomically flat Au(111) film as characterized above. The corresponding sputter deposition conditions were similar to those for the Au(111) film, except that there was no secondary deposition step and that a more careful control of deposition temperature was required in the case of Ag(111) film. To ensure the formation of large, atomically flat terraces the substrate temperature had to be raised to at least above ~100°C. On the other hand, the increase in temperature also increased the probability that the film appearance suddenly turned whitish and cloudy to the eye in the middle of the deposition. Note that Ag films sputtered directly onto mica more easily undergo the same phenomenon. This is why we preferred to grow Ag(111) on Au-precoated mica. The undesirable morphological change, even visible by eye, obviously reflects emergence of some large crystallites capable of causing strong light scattering in the visible region,

as confirmed by STM; hence, huge bumps hundreds of nanometers across and more than tens of ångströms high could be easily located. Although atomically flat terraces do exist in between these bumps, such films cannot be suitable as a substrate for further STM or AFM studies. The upper limit of temperature above which the serious clouding becomes difficult to prevent seemed to be around 200°C. Thus, the best films could be made at temperatures somewhere between 150 and 200°C. A collection of STM images shown in Fig. 3 demonstrates the superior flatness of the Ag(111) films grown in this region, specifically at ~170°C. The hexagonal faceting associated with (111) planes of fcc metals can be seen as the common step pattern on the atomically flat Ag(111) films, though irregularly rounded step edges also coexist in different ratios in different areas. It should be noted, however, that the occurrence of such a distinct hexagonal faceting, though interesting itself and providing additional proof for the (111) orientation, is not necessarily the essential condition for the Ag(111) film to be grown atomically flat. In fact, if one compares the regions imaged in Figs. 3c and d, the latter exhibiting essentially no facet steps at all in the corresponding scan window, it would be difficult to tell which is flatter than the other.

It should also be noted that the surface topographies shown in Fig. 3 are representative of the majority of Ag(111) films grown in the above-noted optimum temperature region. In other words, clearly distinguishable topographic changes from that shown in Fig. 3 became noticeable only at temperatures near or beyond the limits of the optimum region. Fig. 4 shows what typically occurs at these temperatures, e.g. ~120°C (Fig. 4a) and ~200°C (Fig. 4b). The films imaged here still exhibit relatively flat terrace structures along with hexagonal faceting but, unlike the flattest films, a number of deep holes or grooves (typically tens of nanometers across and several nanometers deep) are left on the low-temperature film and considerably rugged terraces appear on the high-temperature sample. As mentioned already, at or above the high temperature limit (~200°C) a more drastic change in the surface

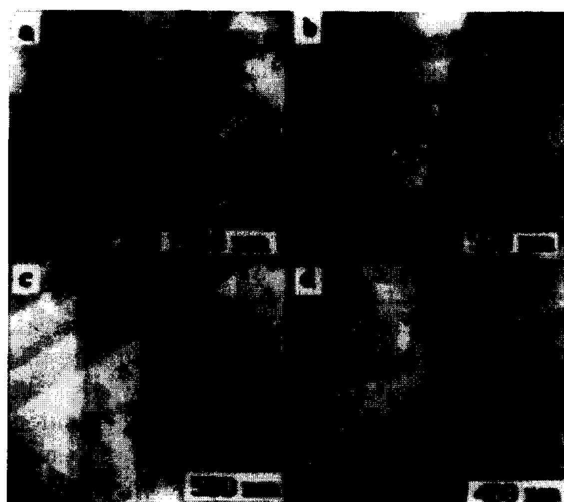

Fig. 3. Collection of STM images taken for the flattest Ag(111) films (~50 nm thick) sputter-grown at ~170°C on the atomically flat Au(111) film predeposited on mica. The apparent maximum height differences are: (a) 4.1 nm, (b) 2.0 nm, (c) 1.9 nm, (d) 1.4 nm.

(a) Ts ~ 120 °C

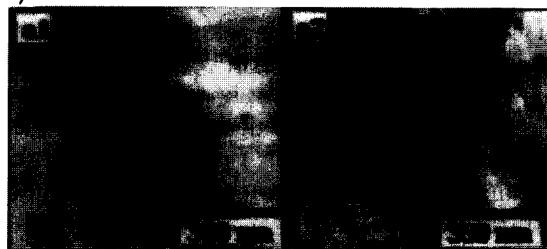

(b) Ts ~ 200 °C

Fig. 4. Topographic features associated with apparently less-flat Ag(111) films grown at temperatures (~120°C and ~200°C) near or beyond the limits of the optimum region. Deep holes (a) or considerably rugged terraces (b) are observed. The apparent maximum height differences, except for the regions of deep holes, are: (a1) 3.2 nm, (a2) 2.4 nm, (b1) 2.7 nm, (b2) 3.1 nm.

topography also sets in easily as a result of the serious clouding of the film surface.

In their recent work on the epitaxial growth of evaporated Ag(111) on mica, Baski and Fuchs were able to prepare Ag(111) films with an extended terrace structure (comparable with that shown in Fig. 3b) only by using such a high deposition rate as ~40 Å s^{-1} at a substrate temperature of ~200°C [14]. In that context they referred to the aforementioned criterion that higher deposition rates produce flatter films. This is again in marked contrast with the fact that we could obtain even flatter films by using the much lower deposition rate of less than 1 Å s^{-1}. This can be another merit of sputter deposition, as lower deposition rates are generally thought to allow easier experimental control over the film growth mode and the resultant surface morphology.

It has been suggested that sputtered atoms may have some large kinetic energy, thus their energetic impact with the growing film surface would cause a poorly oriented pebble-like structure for Au films sputtered onto a room temperature mica [18]. We wonder, however, what fraction of the initial kinetic energy the sputtered atoms could retain when they reach the film surface in the Ar gas atmosphere of ~0.2 Torr. The fact that the substrate is contacting with the discharge plasma in our deposition system may also be an important difference from vacuum evaporation. In addition, the deposition-rate gradation on the substrate mentioned earlier could possibly make some positive contribution in increasing the step density and thus facilitating the step-spreading growth mode [19]. It is interesting to study further how these factors contribute to the growth of atomically flat Au(111) and Ag(111) films in the conditions of the apparently much lower substrate temperature and/or deposition rate than required for evaporated films to attain a similar level of flatness.

References

[1] M. Salmeron, T. Beebe, J. Odriozola, T. Wilson, D.F. Ogletree, W. Siekhaus, J. Vac. Sci. Technol. A 8 (1990) 635.

[2] A. Ikai, Surf. Sci. Rep. 26 (1996) 261.

[3] C.A. Widrig, C.A. Alves, M.D. Porter, J. Am. Chem. Soc. 113 (1991) 2805.

[4] L.A. Bottomley, J.N. Haseltine, D.P. Allison, R.J. Warmack, T. Thundat, R.A. Sachleben, G.M. Brown, R.P. Woychik, K.B. Jacobson, T.L. Ferrell, J. Vac. Sci. Technol. A 10 (1992) 591.

[5] Y.T. Kim, R.L. McCarley, A.J. Bard, J. Phys. Chem. 96 (1992) 7416.

[6] E. Bunge, R.J. Nichols, H. Baumgaertel, H. Meyer, Ber. Bunsenges. Phys. Chem. 99 (1995) 1243.

[7] W. Mizutani, M. Motomatsu, H. Tokumoto, Thin Solid Films 273 (1996) 70.

[8] C.E.D. Chidsey, D.N. Loiacono, T. Sleator, S. Nakahara, Surf. Sci. 200 (1988) 45.

[9] R. Emch, J. Nogami, M.M. Dovek, C.A. Lang, C.F. Quate, J. Appl. Phys. 65 (1989) 79.

[10] A. Putnam, B.L. Blackford, M.H. Jericho, M.O. Watanabe, Surf. Sci. 217 (1989) 276.

[11] J.A. DeRose, T. Thundat, L.A. Nagahara, S.M. Lindsay, Surf. Sci. 256 (1991) 102.

[12] J. Inukai, W. Mizutani, K. Saito, Jpn. J. Appl. Phys. 30 (1991) 3496.

[13] M. Hegner, P. Wagner, G. Semenza, Surf. Sci. 291 (1993) 39.

[14] A.A. Baski, H. Fuchs, Surf. Sci. 313 (1994) 275.

[15] M. Kawasaki, H. Ishii, Langmuir 11 (1995) 832.

[16] M. Kawasaki, H. Ishii, J. Imaging Sci. Technol. 39 (1995) 210.

[17] M. Kawasaki, H. Uchiki, Chem. Phys. Lett. 254 (1996) 98.

[18] Y. Golan, L. Margulis, I. Rubinstein, Surf. Sci. 264 (1992) 312.

[19] K. Meinel, M. Klaua, H. Bethge, Phys. Status Solidi A 110 (1988) 189.